

## Process Optimization and Kinetic study of Wet Peroxide Oxidation of Phenol in Wastewater over Mg-Al Nano Mixed Oxide

Masoud Samandari<sup>a</sup>, Afshin Taghva Manesh<sup>a\*</sup>, Seyed Ali Hosseini<sup>b</sup>, Sakineh Mansouri<sup>a</sup>

*a) Department of Chemistry, Central Tehran Branch, Islamic Azad University, Tehran, Iran*

*b) Department of Applied Chemistry, Urmia University, Urmia, Iran*

Received 12 January 2021; received in revised form 15 May 2021; accepted 16 May 2021

### ABSTRACT

The wet peroxide oxidation (CWPO) of phenol in the polluted water on Mg-Al nano mixed oxide was investigated and the optimization and kinetic of the process were studied. The nanocatalyst was characterized by XRD, FESEM, EDS and BET. The average crystallite size of 25 nm was estimated using Scherrer formula. FESEM images approved the catalyst comprised of spherical nanoparticles in the range of 94-130 nm. BET results indicated the mesoporous nanocatalyst (dpore=21 nm) has a specific surface area of 86.3 m<sup>2</sup>.g<sup>-1</sup>. The optimized conditions of the process resulted at initial concentration of phenol, reaction temperature, reaction time and hydrogen peroxide volume of 100 ppm, 60°C, 55 min and 3 mL, respectively. The phenol degradation under the optimal conditions reached 85%. The result of the kinetic study indicated that the oxidation of phenol over Mg-Al nano mixed oxide follows the pseudo-first-order kinetics with a correlation factor of 0.94. The activation energy of phenol oxidation over the catalyst was determined to be 19.07 kJ.mol<sup>-1</sup>. The Mg-Al mixed oxide is a cheap and green catalyst and could be prove to promising for the CWPO process.

**Keywords:** *Wet peroxide oxidation, Phenol, Mg-Al mixed nanooxide, Kinetic studies, Activation energy*

### 1. Introduction

The release of phenol and phenolic compounds into wastewaters is caused by a variety of chemical and petrochemical processes [1-4]. The phenol is a toxic compound, and its biodegradation is difficult. For phenol removal, different methods such as adsorption, solid-phase extraction (SPE), wet air oxidation (WAO), catalytic wet air oxidation (CWAO), biodegradation, and advanced methods such as electrochemical oxidation, photo-oxidation, ozonation, UV/H<sub>2</sub>O<sub>2</sub>, Fenton reaction, membrane processes, and enzymatic treatment have been reported [5, 6]. The key characteristic of advanced oxidation is that it is carried out in the presence of hydroxyl radicals. Fenton's reaction is the quickest for phenol removal among these methods. Ozonation was also found to be the most cost-effective process. In the case of ozone compounds, single ozonation produced the best results.

UV/H<sub>2</sub>O<sub>2</sub> processes resulted in the highest degradation rate [7].

There are several articles on the use of photodegradation of pollutants [8-11]. For example, Chaimaa EL Bekkali et al. reported on the photodegradation of antibiotic effluent using metal oxide catalysts [12]. The key advantages of photodegradation are complete degradation through light-induced radical generation and the ability to complete the process at room temperature [13, 14].

Since it uses simple equipment and operates at atmospheric pressure and low temperatures, catalytic wet peroxide oxidation (CWPO) as an advanced oxidation process (AOP), can be considered economically viable for wastewater treatment [1, 4, 5]. Unlike photodegradation methods, the CWPO process uses only the activation energy of the process, which is achieved by lowering the temperature below 353 K. As a result, it is a good approach for phenol remediation since it results in complete phenol degradation at lower temperatures [1, 2].

\*Corresponding author.

E-mail address: *Afshintagvamenesh@gmail.com*

(A. Taghva Manesh)

Catalyst properties, like those of other catalytic processes, have an effect on the efficiency of the process. Hosseini et al. reported the use of Ni-Co layered double hydroxides (LDHs) as a nanocatalyst in the CWPO process for phenol degradation. They used response surface methodology (RSM) to optimize the process conditions [2]. To obtain some information about the rate of the reaction, a kinetic analysis of chemical processes is needed. There are a few papers that discuss the kinetics of phenol degradation by the CWPO method [16-18].

In this study, Mg-Al mixed oxide was formed as a green and inexpensive nanocatalyst for phenol degradation using the CWPO process over Mg-Al nano mixed-oxide. The nano catalyst was easily made from inexpensive and environmentally friendly precursors. In addition, the CWPO process is used to optimize and study the kinetics of phenol degradation over Mg-Al nano mixed-oxide.

## 2. Experimental

### 2.1. The Catalyst Preparation

First, Mg-Al mixed oxide is synthesized from the related layered double hydroxide. XRD, FESEM, EDS, and BET were used to characterize the catalyst. The process was then optimized by considering the effective factors, and kinetic studies were completed as a result. The process mechanism was proposed. The Mg-Al nano mixed oxide was generated by calcining Mg-Al layered double hydroxide (Mg-Al LDH).

First, Mg-Al LDHs (molar ratio Mg/Al = 2) were prepared using the co-precipitation process. The following is a common method of synthesis: First, 6.4 g Mg (NO<sub>3</sub>)<sub>2</sub>·6H<sub>2</sub>O and 4.6 g Al (NO<sub>3</sub>)<sub>3</sub>·9(H<sub>2</sub>O) were dissolved in 100 mL deionized water under stirring with the rate of 300 rpm. Then, a solution (100 mL) containing 1.12g Na<sub>2</sub>CO<sub>3</sub> and 4.0g NaOH was added dropwise in the above homogenous solution to get pH to 10. The resulting mixture was mixed under constant magnetic stirring for 3 minutes at ambient temperature. Then the solid was separated by a vacuum filter and washed thoroughly with water and eventually dried overnight at 70 °C. Mg-Al nano mixed oxide was obtained by calcination of the Mg-Al LDH sample at 500 °C for 3h.

### 2.2. The catalyst characterization

The crystalline phase of the catalyst was investigated by X-ray diffraction (PW1800 model of PHILIPS devices) and Cu K<sub>α</sub> radiation (λ= 1.54 Å). A MIRA3 TESCAN instrument was used to determine the morphology of the mixed oxides using field-emission scanning electron

microscopy (FESEM) after pre-coating samples with gold. The distribution of particle size was performed by Image J software. The N<sub>2</sub> adsorption-desorption isotherms were determined using Belsorp Max instrument (BEL Japan, Inc.) The BET (Brunauer–Emmett–Teller) method was used to calculate the specific surface area of the nanocatalyst.

### 2.3. Experimental process

The catalytic tests in catalytic wet oxidation were conducted in a laboratory-scale batch reactor. In all studies, the catalyst dosage and stirring rate kept fixed. To optimize the process, the different values of hydrogen peroxide, reaction time, reaction temperature and initial concentration of phenol in the simulated wastewater were considered. The kinetic study of the process was done by calculating the rates at different concentrations and utilizing different kinetic models. The activation energy of the process was determined using the Arrhenius equation. The concentration of the remaining phenol after the reaction was detected and measured by a UV-Vis spectrophotometer (PG Instrument 80). To investigate the possible by-product produced from degradation of phenol, sampling was done in different times and UV-Vis spectrum of the samples was taken in the range 190-700 nm. If there was any peak in the spectrum, this indicates a by-product.

The percentage of phenol was calculated using the following equation (Eq. 1):

$$R = \frac{[input]-[output]}{[input]} \times 100 \quad (1)$$

## 3. Result and Discussion

### 3.1. sample characterization

#### 3.1.1. XRD characterization

**Fig. 1** represents the XRD pattern of Mg-Al nano mixed oxide. As stated in the experimental section, the mixed oxide resulted from the calcination of Mg-Al LDH (hydrotalcite). Due to the collapse of the structure of Mg-Al-LDHs, the peaks of hydrotalcite disappeared from the pattern, and the broad peaks ascribed to the formation of Mg-Al appeared. After calcination at 500 °C, an Mg(Al)O mixed oxide of low crystallinity with periclase structure (MgO) is generated [JCPDS 75-1525]. The similarity of XRD pattern of Mg-Al mixed oxide with that of MgO indicates that the Al<sup>3+</sup> ions are well dispersed in the MgO lattice without the segregation of AlO<sub>x</sub> crystalline phases [19]. The crystallite size was calculated using Scherrer method [20] according to the Eq. (2).

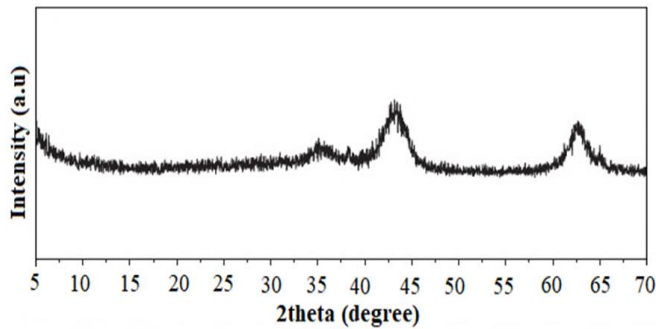


**Fig. 1.** The XRD patterns of calcined LDH (Mg-Al nano mixed oxide).

$$D = \frac{k\lambda}{\beta \cos\theta} \quad (2)$$

According to the Scherer formula, the mean crystallite size was determined as 25 nm.

### 3.1.2. FESEM/EDS analysis

The particle size and morphology of the Mg-Al oxide are investigated by FESEM and the FESEM images are shown in **Fig. 2.a**. It is observed that the catalyst is comprised of agglomerated particles with different sizes in the range 94-130 nm. The distribution of particle sizes resulted by Image J software indicated that the abundant range of particle size was 98-108 nm (**Fig. 2b**). The EDS of the nanocatalyst is shown in **Fig. 2c**. The EDS analysis indicated that the Mg/Al ratio is around 2 and the presence of C and O atoms in the EDS approved the interlayer of  $\text{CO}_3^{2-}$ . The presence of C could be that the degradation of carbonate interlayer was not complete. The sharp peak around 2-3 keV indicates Pt coating.

### 3.1.3. Specific surface area

The nanocatalyst's specific surface area was determined to be  $86.3 \text{ m}^2 \cdot \text{g}^{-1}$ . **Fig. 3** shows the nitrogen adsorption-

desorption of the nanocatalyst. The nanocatalyst's pore size and volume were 21 nm and  $0.45 \text{ cm}^3 \cdot \text{g}^{-1}$ , respectively. The catalyst shows the Isotherm type-III with an  $\text{H}_3$  hysteresis type, meaning that mesopores and macropores are found in the catalyst.

### 3.2. Process optimization

The catalytic oxidation of the phenol process was optimized by taking four major factors into account: initial phenol concentration, reaction temperature, reaction time, and hydrogen peroxide volume. The optimization was carried out using the *one factor at a time* method. In this method of optimization, one factor is optimized at a time while the values of the other factors remain constant. **Table 1** shows the range of factors and the optimum value.

In the optimum conditions, the conversion of the phenol over the catalyst was 85%. Bagheri et al. studied Cu- $\text{Co}_2$  and Cu- $\text{Mn}_2$  for phenol degradation. They concluded that the conversion of phenol was 82% on Cu- $\text{Co}_2$  oxide after 40 min, and it was 78% on the Cu- $\text{Mn}_2$  oxide after 50 min [1]. Massa et al. investigated the CWPO of phenol solutions over CuO/ $\text{CeO}_2$  systems at 70 °C [21]. Zazo et al. also reported the optimum temperature of 50 °C for CWPO of phenol with a Fe/C catalyst [22]. According to Hosseini et al., the maximum phenol degradation over the CoNi LDH resulted under following conditions:  $4.03 \text{ g} \cdot \text{L}^{-1}$ , 77.8 min, 0.5 mL  $\text{H}_2\text{O}_2$ , and 100 ppm (phenol) of catalyst amount, reaction time,  $\text{H}_2\text{O}_2$  volume, and phenol concentration, respectively [2]. So, the optimum value for phenol concentration is in agreement with some papers. In general, the catalyst type and its physical-chemical properties affect the optimum conditions. That is why different optimum conditions are observed in various papers.

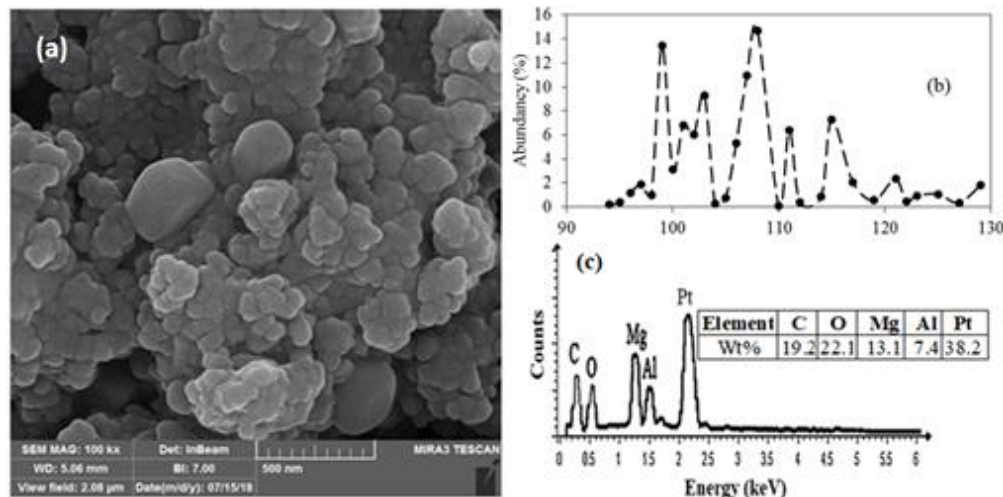


**Fig. 2.** SEM image Mg-Al mixed oxide (a), (b) DLS analysis and (c) EDS analysis

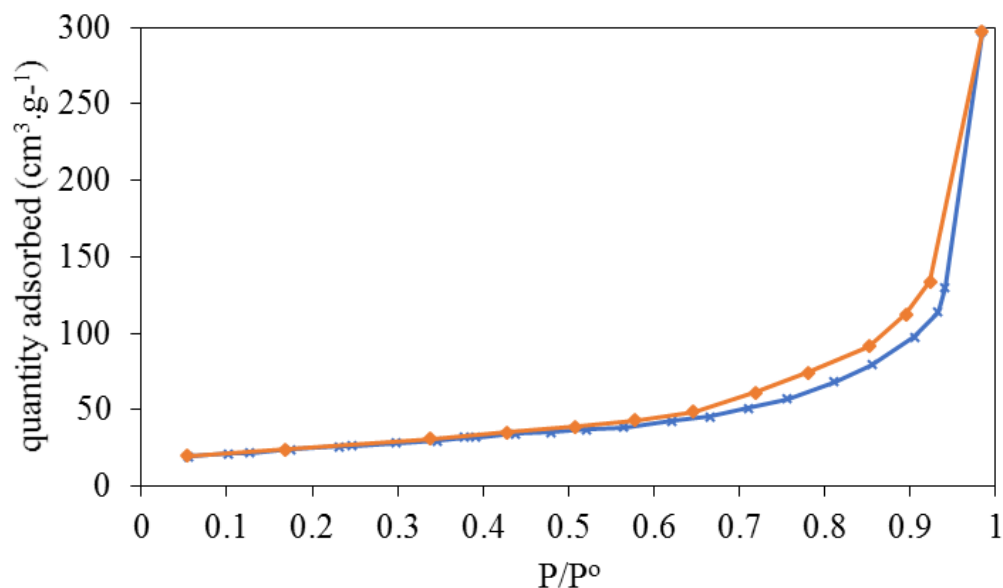


**Fig. 3.** N<sub>2</sub> adsorption-desorption curve of the Mg-Al mixed oxide (T=77 K)

**Table 1.** The optimum value of operation variables

Factor	Range	Optimum value
Initial phenol concentration (ppm)	50-300	100
Reaction temperature (°C)	25-80	60
Times on stream (min)	25-65	55
Hydrogen peroxide volume (mL)	1-5	3

### 3.3. Mechanism of the phenol oxidation over Mg-Al mixed oxide

In the mechanism, first hydrogen peroxide is degraded on the catalyst surface forming hydroxyl radicals. Then, hydroxyl radicals at the catalyst surface react with phenol to produce hydroquinone and catechol as intermediates. Further oxidation results in the transmission of intermediates to maleic acids, oxalic acid and acrylic acid.

All these compounds are considered as intermediates in **Fig. 4**. Finally, the intermediates decomposed to carbon dioxide and water vapor. The proposed mechanism for phenol oxidation over the mixed oxide is shown in **Fig. 4**. Since the OH radical has high potential to oxidize the organic compounds completely to carbon dioxide and water vapor. The mechanism is in agreement with the literature [2, 16, 23].

### 3.4. Kinetic studies

Kinetic studies are needed for any catalytic process. They provide information about the pathways of the reaction. The experimental results were analyzed using two kinetic models: pseudo-first order and pseudo-second order [16, 24]. Different contact times in the range of 25-60 minutes were used in the kinetic model experiments. As shown in **Table 1**, the values of operation variables were kept at their optimum levels. In **Fig. 5**, the results of the experimental removal of phenol using mixed oxide at various contact times are shown. The **Fig. 5a** shows column chart of phenol at different times on streams in the CWPO process. It is shown that the conversion reached 85% after 45 min. After the 45 minutes the removal rate of phenol reached fixed value. The kinetics of the mechanism were studied in this analysis using the pseudo-first-order model and the pseudo-second-order model, which are seen in **Eqs. 3** and **4**, respectively. [16, 24].

$$\log(q_e - q_t) = \log q_e - \frac{K_1}{2.303} t \quad (3)$$

$$\frac{t}{q_t} = \frac{1}{K_2 q_e^2} + \frac{t}{q_e} \quad (4)$$

Where  $q_e$  and  $q_t$  (mg.g<sup>-1</sup>) are the amounts of converted phenol at a time (t).  $K_1$  ((min<sup>-1</sup>) and  $K_2$  (g.mg<sup>-1</sup>.min<sup>-1</sup>) are the rate constant of CWPO process. The results of experimental correlation coefficients for the models are shown in **Fig. 5 (b, c)** and **Table 2**.

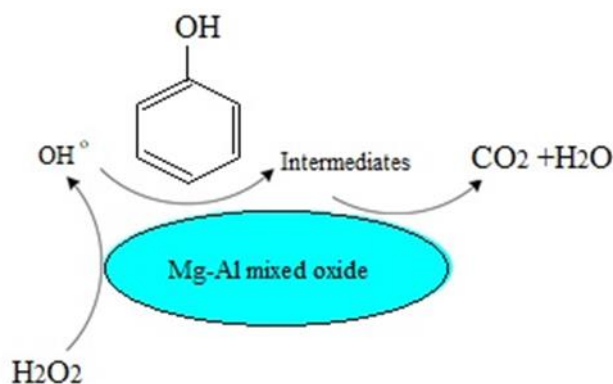


**Fig. 4.** The proposed mechanism for phenol degradation in CWPO process.

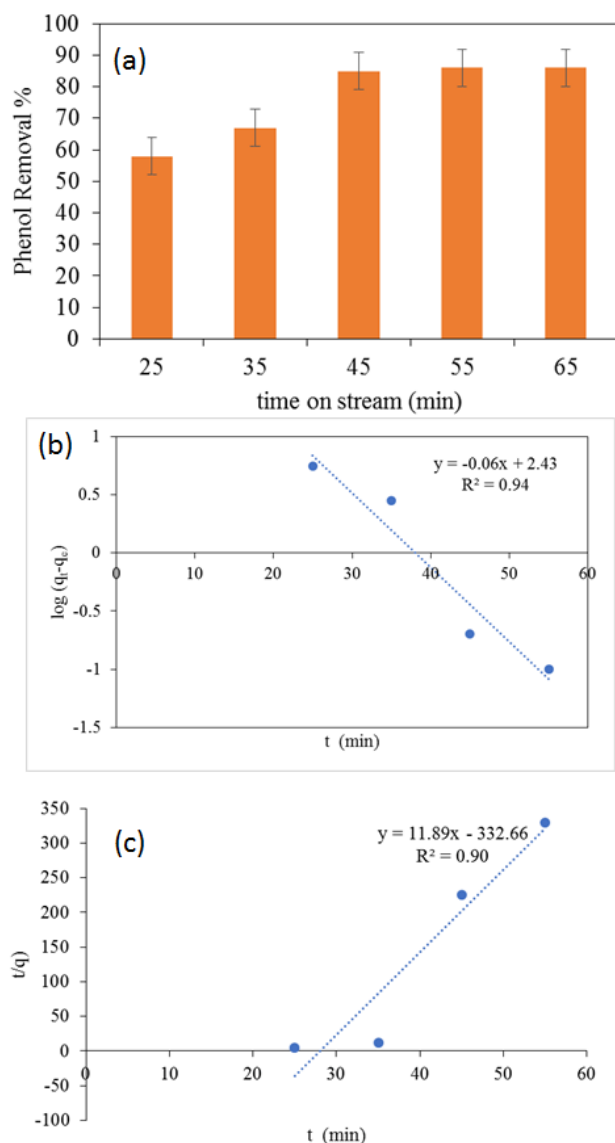


**Fig. 5.** The phenol removal percentage at different times on stream over Mg-Al mixed oxide. (a): The kinetics of phenol oxidation over Mg-Al mixed oxide. The linear fitting for the kinetic equations: b) Pseudo-first-order c) pseudo-second-order. (Condition:  $C_{phenol} = 100$  ppm,  $T = 60$  °C,  $H_2O_2$  volume=3 mL.

According to the correlation coefficients ( $R^2$ ), the kinetics of the phenol oxidation on the catalysts follows from the pseudo-first order kinetic model in that  $R^2$  was 0.94 and more than that of a pseudo-second-order kinetic model (0.90).

### 3.5. Reaction temperature and activation energy

The catalyst particles are dispersed for the generation of hydroxyl radicals by  $H_2O_2$  decomposition over the active sites of catalyst. In addition, it is generally accepted that phenol oxidation is faster during catalytic wet peroxidation processes due to the greater activation of hydrogen peroxide at high temperatures. However, the optimal temperature range is below 350 K to prevent the decomposition of hydrogen peroxide to oxygen and water [1, 21, 22]. The activation energy of the degradation reaction was obtained by plotting data from temperature and  $\ln(k_{app})$  by Arrhenius equation (Eq. 5) [16].

$$k = A \exp\left(-\frac{Ea}{RT}\right) \quad (5)$$

The plot of  $-\ln(k_{app})$  versus the  $1/T$  is shown in Fig. 6. The activation energy of phenol degradation over Mg-Al mixed oxide was determined as 19.07 kJ.mol<sup>-1</sup>. It shows that the catalyst is so active for this process. Rokhina et al. reported the activation energy of 57 kJ.mol<sup>-1</sup> for phenol oxidation over  $RuI_3$  catalyst in the CWPO [25]. Pintar and Levec reported a catalyst comprising ZnO, CuO, and  $Al_2O_3$  for phenol degradation from wastewater. They found activation energy of 84 kJ.mol<sup>-1</sup> in a temperature range of 105 to 130°C for the catalytic oxidation of phenol [26]. The results indicated that Mg-Al mixed oxide is more active than the catalyst reported in literature for phenol degradation by CWPO process.

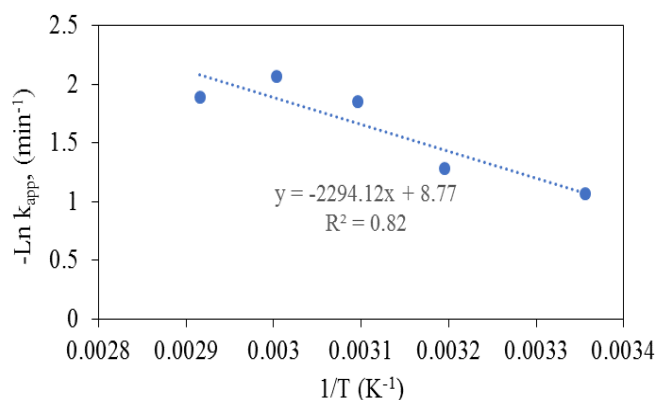


**Fig. 6.** Arrhenius plot for dependence of apparent rate constants to temperature.

**Table 2.** Kinetic constant parameters obtained for removal phenol on Mg-Al mixed oxide.

First-order kinetics			Second-order kinetics			
Catalyst	$q_e$ (mg.g <sup>-1</sup> )	$K_1$ (min <sup>-1</sup> )	$R^2$	$K_2$ (g.mg <sup>-1</sup> .min <sup>-1</sup> )	$R^2$	$q_{e,cal}$ (mg.g <sup>-1</sup> )
Mg-Al mixed oxide	11.36	0.147	0.94	0.42	0.90	0.84

#### 4. Conclusions

The Mg-Al mixed oxide was formed during the calcination of Mg-Al-CO<sub>3</sub> layered double hydroxides at 500 °C. The calcined LDH was in the form of Mg-Al mixed oxide and MgO. The catalytic activity of Mg-Al mixed oxide in the removal of phenol from wastewater by catalytic wet peroxide oxidation was successfully investigated. The Mg-Al mixed oxide exhibited a considerable activity for phenol remediation which is ascribed to the synergetic behavior of MgO and Mg-Al oxide. The conditions of the process were optimized initial concentration of phenol, reaction temperature, reaction time and hydrogen peroxide volume of 100 ppm, 60 °C, 55 min and 3 mL, respectively. The kinetic of the process was followed by a pseudo-first-order. The activation energy of phenol oxidation over the catalyst was determined to be 19.07 kJ.mol<sup>-1</sup>. It is concluded that the catalyst could be promising to be investigated in CWPO process.

**Conflict of Statement:** There is no conflict of the statement in this work.

#### Acknowledgment

The authors are grateful to research deputies of Islamic Azad University-Tehran Central Branch and Urmia University.

#### References

[1] B. Bagheri, S.A. Hosseini, H. Mehrizadeh. *J. Water Environ. Nanotechnol.*, 5 (2020) 139-146.  
 [2] S. A. Hosseini, M. Davodian, A. R. Abbasian, J. Taiwan Inst. Chem. Eng, 75 (2017) 97-104.  
 [3] A. Nezamzadeh-Ejhih, M. Bahrami, Desal. Water Treat. 55 (2015) 1096–1104.  
 [4] Zarifeh-Alsadat Mirian, Alireza Nezamzadeh-Ejhih, Desal. Water Treat. 57 (2016) 16483–16494.  
 [5] N. Pourshirband, A. Nezamzadeh-Ejhih, S. N. Mirsattari, Chem. Phys. Lett. 761 (2020) 138090-138099.  
 [6] B. Divband; A. Jodaie; M. Khatamian, Iran. J. Catal. 9 (2019) 63-70.  
 [7] S. Esplugas, J. Gimenez, S. Contreras, E. Pascual, M. Rodri'guez, Water Res. 36 (2002) 1034–1042

[8] R. Surkatti, M. H. El-Naas, M. C. M. Van Loosdrecht, A. Benamor, F. Al-Naemi, U. Onwusogh, *Biotechnology for Gas-to-Liquid (GTL) Wastewater Treatment: A Review*, *Water* 12(8) (2020) 2126-2152  
 [9] S Mohammadi, A Kargari, H Sanaeepur, K Abbasian, A Najafi, E. Mofarrah, *Desalin Water Treat.* 53 (2015) 2215–34.  
 [10] F. Soori, A. Nezamzadeh-Ejhih, *J. Molecul. Liq.* 255 (2018) 250–256.  
 [11] I. Nowak, I. Rykowska, J. Ziemblińska-Bernart, *J. Iranian Chem Soc.*, 17, (2020) 825–838.  
 [12] C.E. Bekkali, H. Bouyarmane, S. Laasri, A. Laghizil, *A. Iran J. Catal.* 8 (2018) 241-247.  
 [13] M. Giah; A. Hoseinpour Dargahi, *Iran J. Catal.* 6 (2016) 381-387.  
 [14] A. Nezamzadeh Ejhih, M. Khorsandi, *J. Hazard. Mater.* 176 (2010) 629–637  
 [15] H. Derikvandi, A. Nezamzadeh-Ejhih, *J. Colloid Interf. Sci.* 490 (2017) 314–327.  
 [16] O. Gholipoor, S. A. Hosseini, *New J. Chem.*, 45 (2020) 2536-2549.  
 [17] K. Maduna, N. Kumar, A. Aho, J. Wärnå, S. Zrnčević, D. Yu. Murzin, *ACS Omega* 3, 7 (2018) 7247–7260  
 [18] A. Santos, P. Yustos, B. Durban, F. Garcia-Ochoa, *Ind. Eng. Chem. Res.* 40, 13 (2001) 2773–2781  
 [19] J.G Li, T. Ikegami, J.H. Lee, T. Mori, Y. Yajima, *J. Europe Ceram. Soc.* 21 (2001) 139-148  
 [20] M. Balakrishnan, R. John, *Iran. J. Catal.* 10(1) (2020) 1-16.  
 [21] P. Massa, F. Ivorra, P. Haure, R. Fenoglio, *J Hazard Mater* 190 (2011) 1068–1073.  
 [22] J.A. Zazo, J.A. Casas, A.F. Mohedano, J.J. Rodri'guez, *Appl Catal B*, 65 (2006) 261–268.  
 [23] H. Li, X. Yu, H. Zheng, Y. Li, X. Wang, M. Huo, *RSC Adv.* 4 (2014) 7266-7274.  
 [24] T. Kumar, R. Mohsin, Z.A. Majid, M.F.A. Ghafir, A.M. Wash, *Appl Energy*, 259 (2019) 114150-114172.  
 [25] E. V. Rokhina, E. Repo, J. Virkutyte, *Ultrasonic Sonochem* 17 (2010) 541–546.  
 [26] A.Pintar, J.Levec, *J. Catal.*, 135(2) (1992) 345-357